

APPLICATION NOTE

Overview

Pushing device operation frequencies towards sub-THz range causes serious challenges for conventional device characterization techniques. Presently, RF device characterization uses a two-step approach (Fig. 1):

1. Probe-tip calibration (off-wafer) that is performed on a commercially available alumina calibration substrate and uses well-characterized Impedance Standard Substrates (ISS).
2. De-embedding of the silicon back-end parasitics using wafer-embedded test structures such as Open and Short (also called “dummies”).

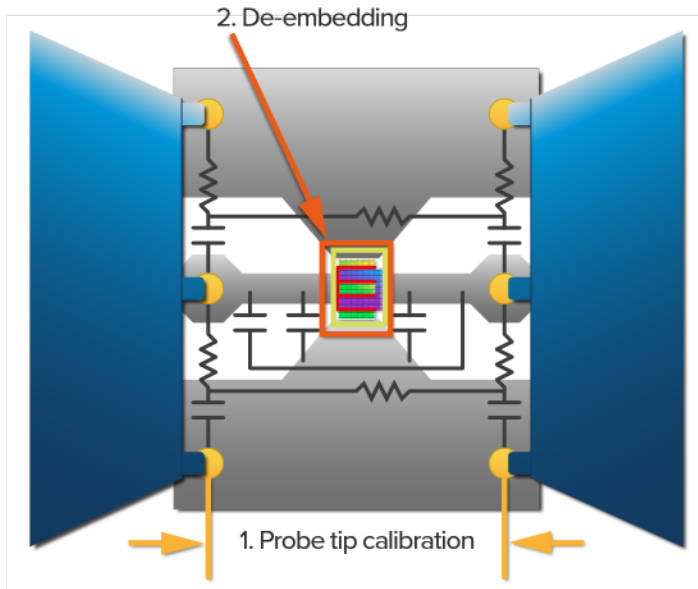


Figure 1. Two-step approach for RF device characterization.

Each dummy is designed to represent a part (series or parallel) of the back-end parasitic impedances. After measurement, these impedances are subtracted by a step-wise procedure yielding characteristics of the device under test (DUT).

A good understanding of possible sources of errors and potential room for improvement at each step, are the key to increase the accuracy of device characterization.

This application note presents a comparison of SOLT, NIST multilayer TRL, and LRRM probe-tip calibration methods for accuracy of measured and extracted figure of merits (FoM) of advanced BiCMOS HBT.

S-Parameter Measurements

Scattering, or S-parameters, are widely used in engineering practice to describe the electrical behavior of a linear network. They are directly measured by a vector network analyzer (VNA) as the relationship between the incident (a), reflected and transmitted (b) by the network (DUT) power waves:

$$S_{11} = \frac{b_1}{a_1}, \quad S_{21} = \frac{b_2}{a_1}$$

where S_{11} is the DUT reflection coefficient at its port 1, S_{21} is the DUT transmission coefficient from port 1 to port 2, a_1 and b_1 are the incident and reflected power waves at the DUT port 1 respectively, and b_2 is the transmitted power wave measured at the DUT port 2.

S-parameters are also related to the DUT impedance Z_{DUT} :

$$S = \frac{Z_{DUT} - Z_{REF}}{Z_{DUT} + Z_{REF}}$$

where Z_{REF} is the measurement reference impedance (typically 50Ω).

Depending on the application needs, S-parameters can be easily converted to various other DUT characterization parameters such as Z, Y, H, ABCD, etc [1].

Calibrating the VNA is an essential step that must be completed before doing any S-parameter measurements. The goal of the calibration is to define systematic measurement errors that will be further excluded from the DUT measurement results by the error correction procedure. In other words, the calibrated system has a virtual measurement reference plane located close to the DUT (at the probe tip end) and has an accurately-defined reference impedance Z_{REF} .

Modeling of Systematic Measurement Errors

There are different methods of describing systematic measurement errors of the VNA, or so-called “error models.” The number of error coefficients included in the model depends on the hardware topology of the VNA, the number of VNA ports and measurement receivers and the required measurement accuracy.

There are two models that are commonly used in practice for a 2-port VNA: 10-term and 7-term. The majority of modern VNAs

realize a so-called double-reflectometer architecture (Fig. 2): each measurement port is associated with two measurement receivers for detecting incident and reflected (transmitted) power waves. Such an architecture can be modeled by both 10-term and 7-term error models. The 7-term error model enables application of advanced, self-calibration methods which specifically benefit wafer-level measurements.

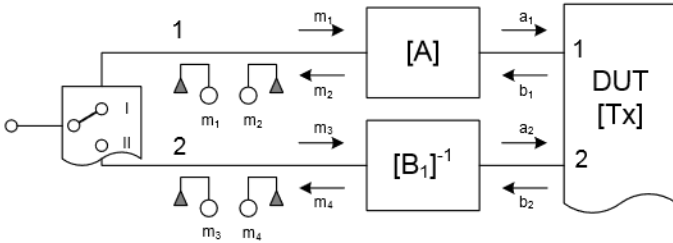


Figure 2. Double-reflectometer VNA.

The 7-term model (Fig. 3) virtually represents the measurement system as an ideal VNA and is a cascaded connection of the imagine error 2x2 matrices [A] and [B] and the DUT [Tx] in transmission or T-parameters representation. It was shown that one of eight error terms (typically A_{21}) can be set as a free parameter, therefore only seven terms must be defined by calibration procedure.

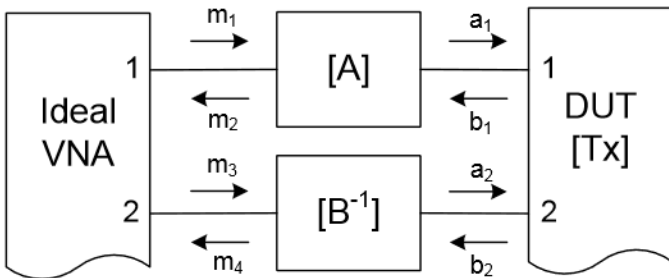


Figure 3. 7-term error model.

A simplified VNA architecture shares one reference receiver between all measurement ports (Fig. 4). Systematic errors of such VNAs are described by the 10-term error model (Fig. 5) and have limited selection of calibration algorithms. The 10-term error model is built on the S-parameter signal flow diagram. It counts five coefficients for each measurement direction: forward and reverse.

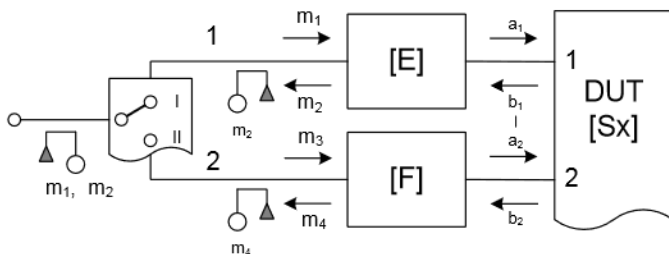


Figure 4. Reference channel VNA.

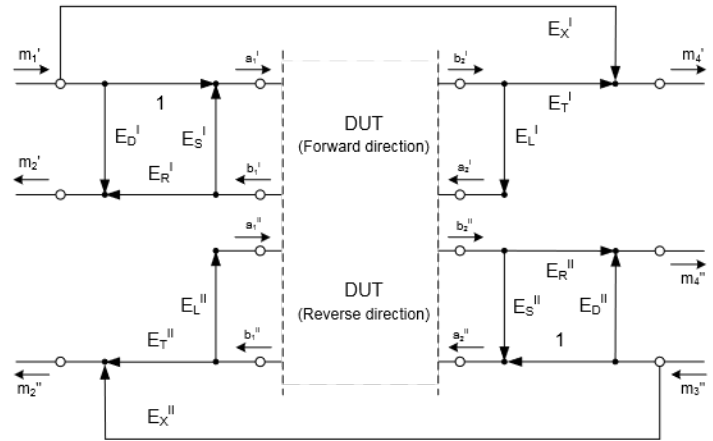


Figure 5. 10-term error model.

Impact of Probe Placement on Calibration Standards

In contrast to the coaxial applications, electrical characteristics of planar calibration standards, such as equivalent impedance and electrical length (Fig. 6), are sensitive to the placement of wafer probes. For instance, the equivalent reactance of the coplanar Load can vary depending on how the standard is contacted: at its beginning, at the middle or at the end (Fig. 7).

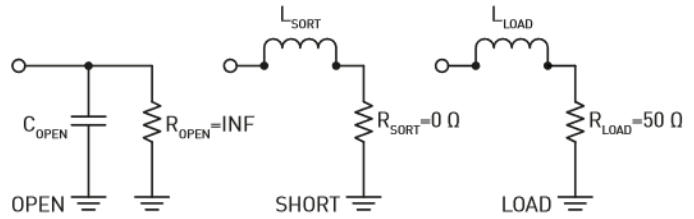


Figure 6. Equivalent circuits of the planar Open, Short and Load standards.

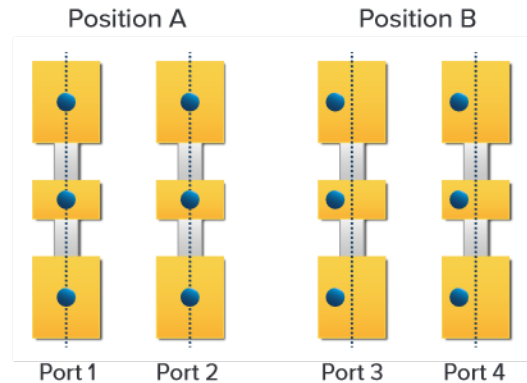


Figure 7. Various positions of the probe tip on the planar Load standard.

Because Load plays a crucial role in many calibration methods defining the measurement reference impedance Z_{REF} , such unpredictable variation of the Load impedance (e.g. Load inductance, Fig. 8) can lead to the unknown calibration reference impedance, resulting in measurements results which are difficult to interpret.

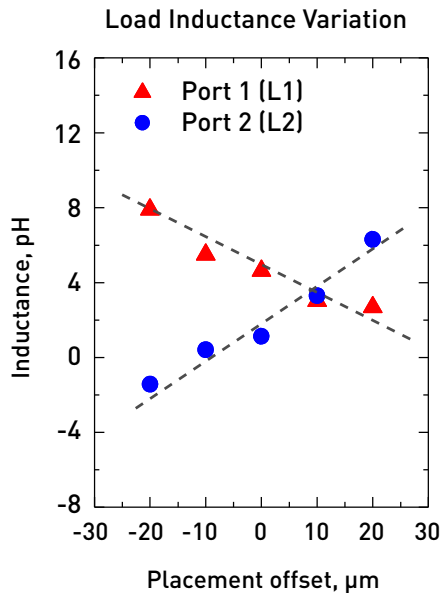


Figure 8. Load inductance variation.

Calibration Methods

In this application note, three calibration methods were evaluated: SOLT, eLRRM, and the NIST multi-line TRL (or mTRL). These methods have the widest variation from each other in:

- 1) systematic error models on which they are built;
- 2) types of required calibration standards;
- 3) definition of calibration reference impedance Z_{REF} ;
- 4) sensitivity to non-ideal standards.

Calibration method: SOLT

SOLT requires three reflection standards at each VNA measurement port (highly-reflective elements, such as Open and Short, and the well-matched $50\ \Omega$ Load) and one transmission standard Thru. All electrical characteristics of standards must be fully known. As a result, the calibration accuracy critically depends on the fabrication and characterization of standards. It remains a challenge to achieve reliable SOLT calibration at high frequencies.

SOLT method is derived for the 10-term error model and can be applied for both the reference channel and double-reflectometer VNA architectures.

Self-calibration methods: eLRRM and multi-line TRL

The evaluated self-calibration methods are based on the 7-term model of systematic measurement errors. They take more measurements of calibration standards than required for

calculating error terms. The gained information redundancy enables the use of partly-defined standards. The missing parameters are calculated from within the calibration procedure (also called “self-calibration”).

Enhanced LRRM

eLRRM method uses one transmission (Thru) and two highly-reflective elements: Reflect (Open) Reflect (Short) measured at both VNA ports. The reflection coefficients of both Reflects are free parameters. This is an important advantage: there is no more need for a well-defined highly reflective element. So far, this has been a challenging task for a wafer-level calibration, especially at high frequencies.

Additionally, eLRRM requires only one Load standard [2, 3]. The eLRRM feature of automatic Load inductance extraction minimizes the calibration error caused by possible probe misplacement on the Load which can lead to inconsistent variation of the Load reactance and, finally, inaccurate detection of the measurement reference impedance Z_{REF} . The algorithm of auto-determination of the Load inductance demonstrated reliable results for the well-defined probe-tip calibration conditions (e.g. on alumina ISS) [4].

Multi-line TRL

TRL relies on the measurement of sections of transmission lines and does not require any definition of the impedance of the Reflect element. The multi-line TRL was developed at NIST to solve the frequency limitation of the conventional TRL procedure [5]. Operating with many lines, it applies an extensive statistical analysis of the redundant information. In conjunction with the method proposed [6], this procedure allows for precise setting of the calibration reference impedance Z_{REF} to $50\ \Omega$ for coplanar calibration on alumina. Therefore, it becomes the accuracy benchmark for comparing different wafer-level calibration schemes [7].

Experimental Results

The experimental measurements were carried out on a broadband S-parameter measurement system from FormFactor consisting of a PM8 manual probe station, $100\ \mu\text{m}$ pitch Infinity Probes®, a matching ISS calibration substrate, and a PNA network analyzer from Agilent Technologies (Fig. 9). The specially designed ceramic AUX site of the RF chuck carried the ISS and suppressed possible influences of parasitic coupling and radiation effects which were increasing with the frequency.

The calibration and error correction were performed for the same data set outside the VNA on a computer. WinCal XE™,

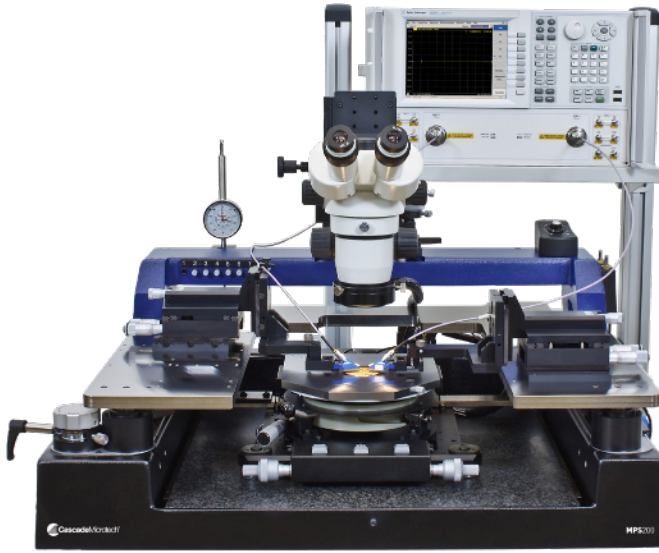


Figure 9. S-parameter measurement test setup with Agilent PNA.

MultiCal and a proprietary IC-CAP[®] script were used for this purpose, while device parameters were extracted using IC-CAP. Offline error correction applied on the same data set excluded the impact of the contact repeatability error as well as the test instrument drift on the comparison results. Therefore, the observed variation in the extracted parameters of the DUT can be attributed to the calibration methods.

The propagation constant γ and the characteristic impedance Z_0 of the ISS lines were extracted using the method from Williams and Marks. This resulted in a capacitance per unit length of $C=1.481$ pF/cm. The reference impedance of the multi-line TRL was set back to 50Ω and the measurement reference plane was moved to the probe tip ends. After that, multi-line TRL established well-defined calibration conditions and could be used as the accuracy benchmark.

Verification of passive elements

The first verification measurements were obtained for the Pad Open de-embedding element. This element is designed to represent parasitic admittance of the DUT contact pad and it is often used in the multi-step de-embedding procedures.

Raw measurement data of the element were calibrated by the probe-tip SOLT, eLRRM and the multi-line TRL methods. The Table 1. Table and extracted parameters of Open, Short and Load standards.

	Open C, fF	Short L, pH	Load L, pH Port 1	Load L, pH Port 2
Table value	-7.2	5.0	-3.3	-3.3
Extracted value	-5.5	6.0	0.1	1.0

equivalent conductance G_1 was extracted from the Π -equivalent circuit (Fig. 10).

The table values of parasitic inductances and capacitances

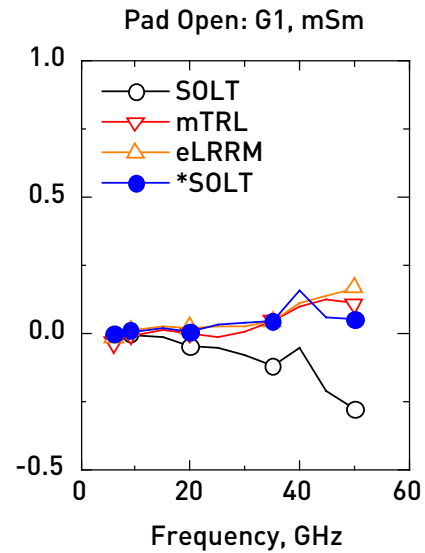


Fig 10. Equivalent conductance G_1 of the pad Open element.

were used for electrical models of calibration Open, Short, Load standards for SOLT calibration method. Both eLRRM and mTRL do not require these definitions.

Both mTRL and eLRRM show expected results, whereas SOLT demonstrate unphysical behavior of the G_1 : it is decreasing with the frequency and becomes negative above a few GHz. This is obviously a calibration artifact. Such artifacts typically illustrate that the calibration reference impedance Z_{REF} was defined incorrectly. In most cases, it is caused by a mismatch of the actual impedance of calibration standards and the table values used for SOLT calibration.

Because eLRRM does not require definition of Open, Short and Load impedances, the actual impedance of these standards can be extracted from the eLRRM-corrected measurement results. Table 1 shows the comparison between the table values and the extracted values for Open, Short and Load.

SOLT calibration was repeated using new parameters for standards. The new SOLT-corrected conductance $G1$ of the Pad Open element is now in good agreement with the reference mTRL calibration.

Verification for a transistor

The most important property of an active device is its capability to provide power gain. Power gain of a transistor decreases with the frequency. The point at which it intercepts the X-axis (equals to unity) is defined as f_{MAX} . Since an active device cannot oscillate if it does not provide power gain, f_{MAX} has been historically called as *maximum oscillation frequency* of a transistor.

f_{MAX} is very sensitive to transistor backend parasitic, as well as to measurement and calibration artifacts. That is why f_{MAX} is a good Figure-of-Merit (FoM) for comparing the impact of different calibration schemes on parameters of active devices.

An HBT with 14.86 μm emitter length and 0.12 μm emitter stack width was chosen as an active verification element. Its S-parameters were measured using different bias conditions

in hot-S (active) mode for $V_B=0.7\text{V}\dots 1\text{V}$ and $V_{CB}=0\text{V}$ (emitter grounded in both cases). The probe-tip calibration was followed by the two-step Open-Short de-embedding of backend parasitics. The Complete Open and Complete Short de-embedding dummy elements are optimized to the specifics of the transistor layout. f_{MAX} was extracted from the Mason's gain (Fig. 11).

f_{MAX} extracted from the mTRL and eLRRM are 297 GHz and 295 GHz respectively. Similar to the results for a passive element, SOLT demonstrated mismatch to both the reference mTRL and eLRRM, and overestimated f_{MAX} for about 27 GHz (or about 10%) compared to the reference value. After the correction for the standards parameters, SOLT-based results are in good agreement with reference calibration methods.

As the second FoM, the maximum frequency at which the transistor demonstrates useful current gain f_T was extracted using the spot frequency method. For this parameter, SOLT underestimated results by 6 GHz (about 3%) compared to the value of 241 GHz for mTRL and eLRRM (Table 2).

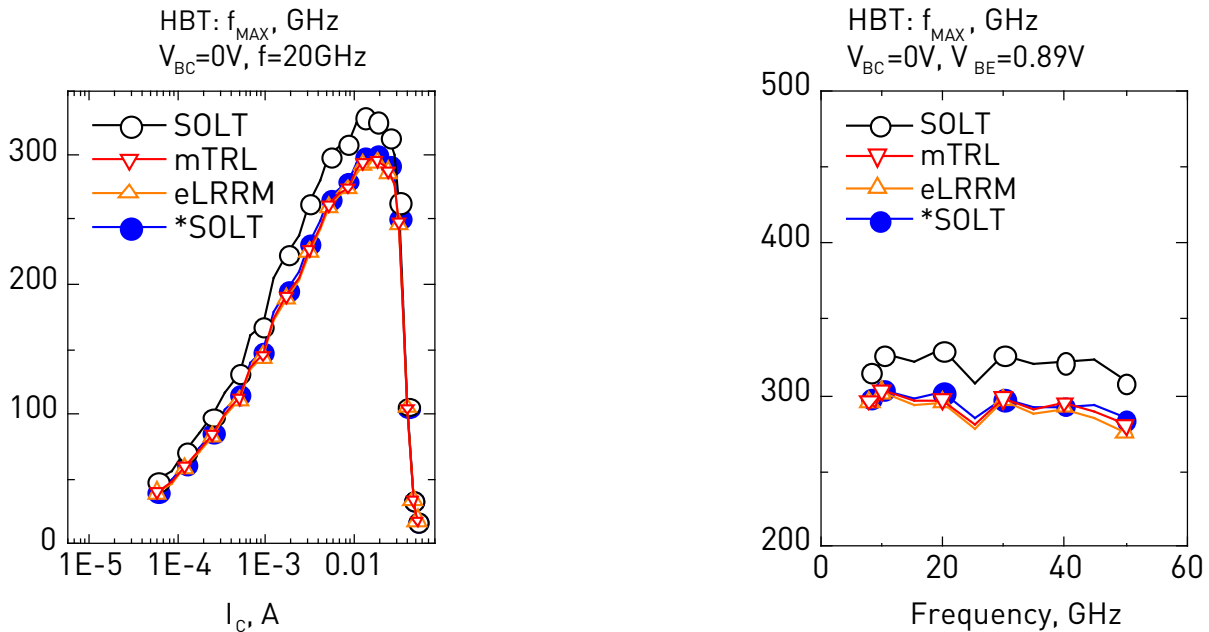


Figure 11. Maximum oscillation frequency f_{MAX} of a test HBT extracted from 20 GHz measurements for different bias conditions (left) and for a fixed bias condition (right) for SOLT, reference NIST multi-line TRL and eLRRM calibration methods. The figure also shows the results for the corrected

Table 2. Extracted FoM f_{MAX} and f_T of test transistor.

	SOLT	*SOLT	mTRL	eLRRM
f_{MAX} , GHz	329	302	297	295
f_T , GHz	236	242	241	241

Conclusion

Inaccurate probe tip calibration affects important FoM of an active device such as f_T and f_{MAX} . Due to the probe misplacement error, SOLT overestimated f_{MAX} by about 10% and underestimated f_T by about 3%. Both reference NIST multi-line TRL and eLRRM provided comparable results for given equal conditions [9].

The undertaken experiments revealed that advanced calibration methods such as multi-line TRL and eLRRM improve measurement accuracy of the small-signal parameters of high-performance devices and significantly outperform conventional SOLT already at lower frequencies, e.g. 20 GHz. The multi-line TRL and eLRRM methods are less susceptible to calibration errors caused by inaccurate probe placement on calibration standards. Although both methods are comparable, eLRRM is much simpler to implement: it does not need re-adjustment of the probe distance, as all standards have the same space and additional procedures for measurement of characteristic impedance Z_0 of the Line are not required.

That is why eLRRM is recommended as an accurate, consistent and easy to implement probe tip calibration method for characterization of advanced high-performance active devices.

References

[1] D. M. Pozar, *Microwave engineering*, 3rd Edition ed.: John Wiley & Sons, Inc.,

2004.

- [2] A. Davidson, K. Jones, and E. Strid, "LRM and LRRM calibrations with automatic determination of load inductance," in *ARFTG Microwave Measurements Conference-Fall*, 36th, 1990, pp. 57-63.
- [3] L. Hayden, "An enhanced Line-Reflect-Reflect-Match calibration," in *ARFTG Microwave Measurements Conference-Spring*, 67th, 2006, pp. 143-149.
- [4] A. M. E. Safwat and L. Hayden, "Sensitivity analysis of calibration standards for fixed probe spacing on-wafer calibration techniques," in *Microwave Symposium Digest, 2002 IEEE MTT-S International*, 2002, pp. 2257-2260.
- [5] R. Marks and K. Phillips, "Wafer-level ANA calibrations at NIST," in *ARFTG Microwave Measurements Conference-Fall*, 34th, vol. 16, 1989, pp. 11-25.
- [6] D. F. Williams and R. B. Marks, "Transmission line capacitance measurement," *Microwave and Guided Wave Letters, IEEE*, vol. 1, pp. 243-245, 1991.
- [7] D. F. Williams, R. B. Marks, and A. Davidson, "Comparison of on-wafer calibrations," in *ARFTG Microwave Measurements Conference-Fall*, 38th, vol. 20, 1991, pp. 68-81.
- [8] Agilent IC-CAP Device Modeling Software, Technical Overview, Agilent Technologies, Inc., 2012
- [9] A. Rumiantsev, P. Sakalas, N. Derrier, D. Celi, and M. Schroter, "Influence of probe tip calibration on measurement accuracy of small-signal parameters of advanced BiCMOS HBTs," in *Bipolar/BiCMOS Circuits and Technology Meeting (BCTM)*, 2011 IEEE Atlanta, GA, 2011.